Available online at www.sciencedirect.com
SCIENCE DIRECT®
Aerosol Science 36 (2005) 1373–1386
Journal of Aerosol Science
www.elsevier.com/locate/jaerosci

Use of porous foam as the substrate of an impactor for respirable aerosol sampling

Cheng-Hsiung Huang[a], Chen-Shen Chang[b], Sheh-Hsun Chang[b], Chuen-Jinn Tsai[b,*], Tung-Sheng Shih[c], Da-Toung Tang[c]

[a]*Department of Environmental Engineering and Health, Yuanpei University of Science and Technology, Hsinchu, Taiwan*
[b]*Institute of Environment Engineering, National Chiao Tung University, No. 75, Poai Street, Hsinchu 300, Taiwan*
[c]*Institute of Occupational Safety and Health, Council of Labor Affairs, Taipei, Taiwan*

Received 20 October 2004; received in revised form 11 March 2005; accepted 14 March 2005

Abstract

The effect of a porous foam substrate on the penetration characteristics of an impactor with a single round nozzle was investigated experimentally, with liquid and solid particles in the size range of 1–10 μm. The experimental results show that the cut-off aerodynamic diameter of the impactor with porous foam substrate is lower than that with porous metal substrate due to more air penetration into the porous foam; in addition, the impactor penetration curve is less sharp. A numerical simulation of the penetration curve for the impactor with porous foam substrate was in good agreement with the experimental data. The numerical method was then used to find the best sampling flow rate for respirable aerosol sampling. Results show that when the nozzle diameter is 0.36 cm and the sampling rate is 1.9 l/min, the penetration curve of the impactor with the porous foam is very close to the criteria for respirable aerosol sampling.

Keywords: Impactor; Single-round nozzle; Porous foam; Respirable aerosol sampler

1. Introduction

Many inertial impactors have been designed and used to measure the size distribution of particles in different environments. To evaluate the health hazard of airborne particles in the workplace, respirable

* Corresponding author. Tel.: |fax: +886 3 5731880.
E-mail address: cjtsai@mail.nctu.edu.tw (C.-J. Tsai).

0021-8502/$ - see front matter © 2005 Elsevier Ltd. All rights reserved.
doi:10.1016/j.jaerosci.2005.03.008

aerosol samplers are often used. The size-selective characteristics of the respirable aerosol samplers have been defined by the American Conference of Governmental Industrial Hygienist (ACGIH), International Organization for Standardization (ISO), and Comite' European de Normalisation (CEN) (Hinds, 1999). Cyclones are often used for respirable aerosol samplers because their penetration curves are less sharp than those of impactors and are close to the respirable sampling convention (Hinds, 1999; Tsai, Shiau, Lin, & Shih, 1999). In addition, cyclones have practical advantages of minimal particle bounce and re-entrainment, and a large capacity for high particle loading (Cohen & Hering, 1995).

In the literature, impactors are also employed as pre-classifiers for respirable aerosol sampling (Lilienfeld & Dulchinos, 1972; Tomb & Treaftis, 1975; Marple, 1978; Willeke & Haberman, 1980; Marple & McCormack, 1983). Some of these investigators had special designs for their impactors to make the penetration curves less sharp and approach the criteria for respirable aerosol sampling. For example, Lilienfeld and Dulchinos (1972) designed a single-stage impactor for respirable dust monitoring at a flow rate of 2 l/min using beta attenuation technology for sensing the mass of the deposited particles. Tomb and Treaftis (1975) used a solid plate impactor inserted with a circular lip to degrade the collection efficiency for respirable sampling. Marple (1978) designed a multiple-nozzle impactor with nozzles of different sizes for simulating the given respirable penetration curve. He demonstrated the feasibility of designing an impactor with respirable penetration characteristic at a flow rate of 28.3 l/min with three nozzle sizes. Respirable penetration curves have also been simulated by impacting a jet on an inclined impaction plate located at several jet-to-plate distances (Willeke & Haberman, 1980). Results showed that when the jet-to-plate distance was about 10, the respirable penetration characteristics could be simulated by the inertial impactor. Porous substrates with oil impregnation were also used as the impaction plate. Marple and McCormack (1983) developed a personal impactor with different nozzle sizes to approximate the respirable penetration curve. They used porous impaction plate impregnated with mineral oil as the substrate to prevent particle bounce.

Recently, polyurethane foams (PUF) were introduced as substrates for conventional inertial impactors (Kavouras, Ferguson, Wolfson, & Koutrakis, 2000; Kavouras & Koutrakis, 2001; Demokritou, Kavouras, Ferguson, & Koutrakis, 2002). The use of PUF substrates overcomes several problems of the traditional inertial impactors such as particle bounce, re-entrainment, or particle over-loading. In addition, adhesive coating on the PUF substrate is not needed and interference with chemical analysis by the coating can thus be avoided. Thus, the impactors with PUF substrates have been used extensively to characterize the physicochemical and toxicological properties of atmospheric aerosols (Kavouras et al., 2000; Demokritou et al., 2002). However, compared to the conventional substrate, the use of PUF as the substrate of an impactor causes significant changes in particle collection efficiency curve. For example, Kavouras and Koutrakis (2001) investigated the collection efficiency of an inertial impactor with PUF substrate as a function of PUF density, Reynolds number (*Re*), impaction substrate diameter, and jet-to-plate distance. Results show that there is a substantial shift of collection efficiency curve to the left of the conventional flat impaction substrate. The sharpness of the collection efficiency curve of the impactor increases with an increasing *Re*. The shift of the cutoff diameter and sharpness change of the collection efficiency curve are attributed to air penetration into the porous substrate (Tsai, Huang, Wang, & Shih, 2001; Huang, Tsai, & Shih, 2001; Huang & Tsai, 2003; Marjamaki & Keskinen, 2004; Demokritou, Lee, & Koutrakis, 2004).

Although cyclones have been used in respirable aerosol sampling for many years, use of impactors as respirable samplers has following advantages. First of all, impactors of different cut sizes can be arranged as a cascade impactor for size-classified aerosol sampling, while cyclones are usually used as a single stage sampler only, such as respirable aerosol sampler. Cascading cyclones of different cut sizes

is difficult. Another characteristic of impactors is that particle samples are collected on the impaction substrates so that subsequent mass and chemical analysis are possible. In comparison, cyclones usually remove particles on the inner wall, which are hard to retrieve for further particle characterization.

In this study, we first determined the penetration curves of liquid particles for a single-round nozzle impactor with two different porous substrates experimentally, porous foam and porous metal substrates. Solid KCl particles were also used to test if particle bounce occurs on porous foam substrates and whether loaded particle mass on the substrates influences the collection efficiency. An empirical equation of particle penetration for the impactor with porous foam was then obtained by fitting the experimental data. Finally, numerical simulation of impactor penetration curve was conducted to find the best sampling flow rate for matching the respirable penetration curve.

2. Experimental method

The schematic diagram of the impactor with porous substrate is shown in Fig. 1. Table 1 lists the design parameters of the impactor with porous foam and porous metal disc. Two nozzles were used in this study including Type I: the nozzle diameter of 0.26 cm (W), the nozzle throat length of 0.26 cm (T), and the jet-to-plate distance of 0.52 cm (S); and Type II: $W = 0.36$ cm, $T = 0.36$ cm, and $S = 0.36$ cm, respectively. Porous foams (diameter: 1.2 cm, thickness: 0.3 cm, SIF: Fine 100 ppi, Foamex Inc., PA, USA) or porous metal discs (diameter: 1.2 cm, pore size: 20 μm, thickness: 0.317 cm, P/N 1000, Mott Corp.,

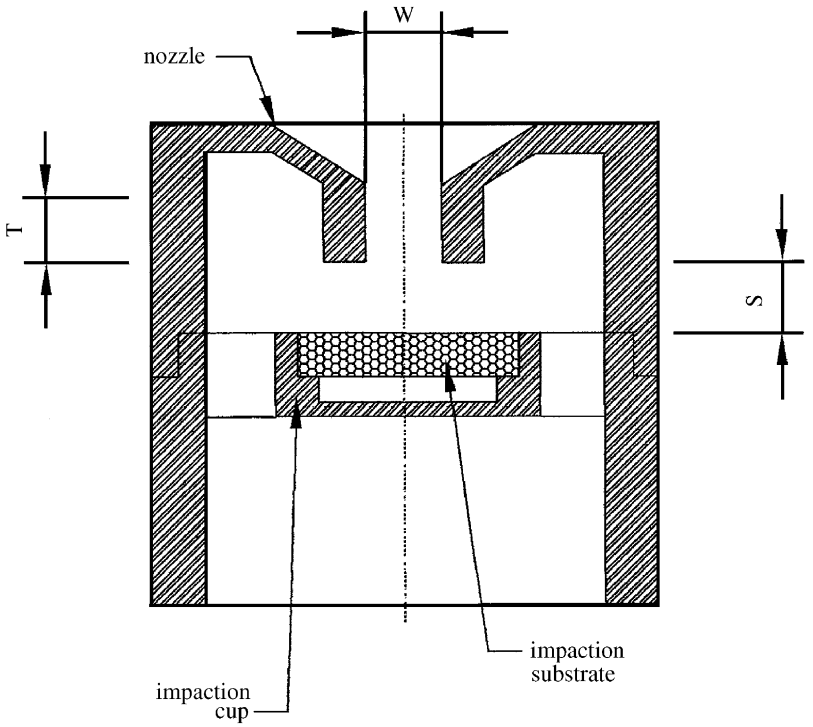

Fig. 1. Schematic diagram of the impactor with porous substrate.

Table 1
The design parameters of the impactor with porous substrate

Nozzle diameter (cm)	Jet-to-plate distance (cm)	Nozzle throat length (cm)	Flow rate l/min	Impaction substrate	Substrate diameter (cm)
0.26	0.52	0.26	1.5	PF[a]	1.2
				PMD[b]	1.2
			2.0	PF	1.2
				PMD	1.2
0.36	0.36	0.36	2.0	PF	1.2
				PMD	1.2
			2.5	PF	1.2
				PMD	1.2

[a]Porous foam.
[b]Porous metal disc.

Farmington, USA) were used as impaction substrates. Particle wall loss in the impactor was determined first using monodisperse oleic acid particles tagged with fluorescein, which were generated by the TSI Model 3450 vibrating orifice monodisperse aerosol generator (TSI Inc., St. Paul, MN, USA). The generated aerosols were neutralized by using a TSI Model 3054 Kr-85 charge neutralizer before the test. An aerodynamic particle sizer (APS, TSI Model 3310A) was used to check the monodispersity and steadiness of the test particles. At the end of each sampling period of 5 min, particles on the impaction substrate, the downstream filter, and the other portions of the impactor were extracted by using 0.001 N NaOH. A fluorometer (Model 10-AU, Turner Designs, CA, USA) was used to measure the wall loss of the impactor, Loss (%), which was determined as

$$\text{Loss}\,(\%) = \frac{M_o}{M_s + M_f + M_o} \times 100\%, \tag{1}$$

where M_s, M_f, and M_o are the mass of fluorescein on the impaction substrate, the downstream filter, and the other portions of the impactor.

After the particle loss test, the particle penetration of the impactor with porous substrate was then measured. The particle loss test is important to this study since particle penetration is to be measured by the real-time instrument, TSI APS. The penetration data are valid only when particle loss is shown to be small. The experimental setup is shown in Fig. 2. Both oleic acid and KCl particles with the aerodynamic diameter ranging from 1 to 10 μm were generated by using an ultrasonic atomizing nozzle (Ultrasonic nozzle, Model 8700, Sono-Tek Inc., NY, USA). Solid KCl particles were used to test if particle bounce occurs on the PF substrate and whether loaded particle mass on the substrate influences the collection efficiency. The aerosols were dried in the upper section of the test chamber by mixing with dried filtered air and were further neutralized by using a TSI Model 3012 Kr-85 charge neutralizer in the middle section of the test chamber. The TSI Model 3310A aerodynamic particle sizer (APS) was used to measure the aerosol number concentrations at the inlet and outlet of the impactor installed in the lower section of the test chamber to determine the particle penetration. The test chamber was made of acrylic material. The outside diameter was 40 cm and the total height was about 230 cm. The inlet aerosol number concentration (N_1) was sampled at a flow rate from 1.5 to 2.5 l/min without the impaction substrate in the impactor

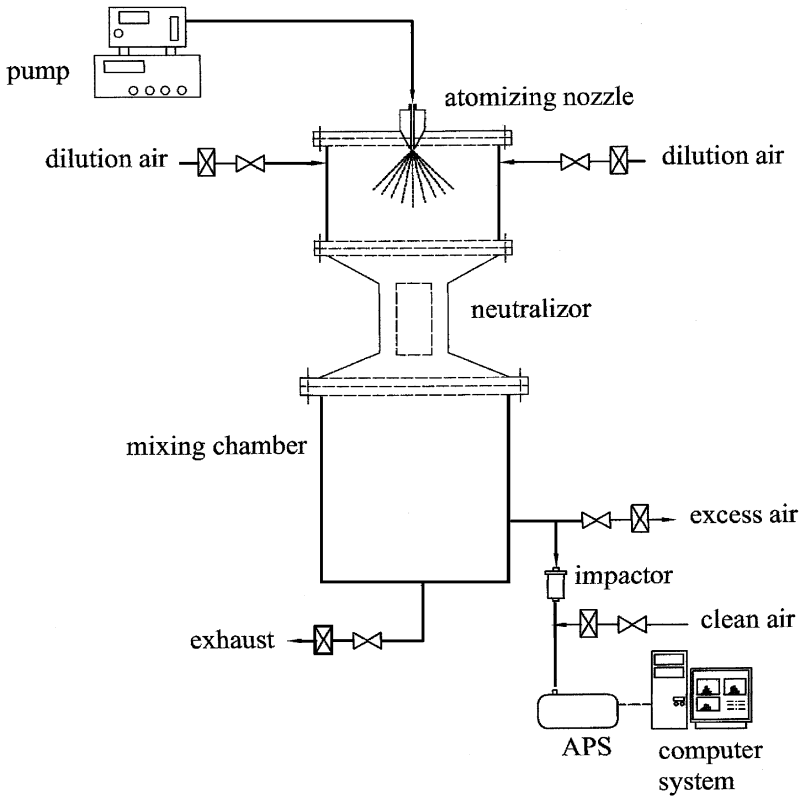

Fig. 2. Experimental setup for the particle penetration of the impactor with porous substrate.

first. An additional 2.5–3.5 l/min of clean air was added to make the total flow rate equal to 5.0 l/min for the APS. The outlet aerosol number concentration (N_2) was determined by the APS when the impaction substrate was put in place in the impactor using the same sampling flow rate as the inlet concentration measurement. After the outlet concentration had been measured, the inlet concentration was measured again to check the steadiness of aerosol concentration. The steadiness was found to be within ±5%. One data point at a particular test condition and particle size is the average of six measurements. The penetration of the impactor with porous substrate, Pen (%), was determined as

$$\text{Pen}\ (\%) = \frac{N_2}{N_1} \times 100\%. \tag{2}$$

The experimental data of particle penetration of the impactor were fitted by the following expression (Kavouras & Koutrakis, 2001):

$$\text{Pen}\ (\%) = A_1 + (A_2 - A_1)[1 + \mathrm{e}^{(D_\mathrm{p} - A_3)/A_4}]^{-1}, \tag{3}$$

where D_p is the particle diameter; A_1, A_2, A_3 and A_4 are regression constants. This equation was used to obtain the theoretical particle penetration of the porous foam as shown in the next section.

In the loading test of solid particles, the loaded mass (mg) of KCl particles on the porous foam of the impactor was determined as

$$\text{Loading mass} = \sum_{j}^{m} \sum_{i}^{n} M_{i,j} \cdot \text{Eff}_{i,j} \cdot \rho_{\text{p}} \frac{\pi D_{\text{p}i}^3}{6}, \tag{4}$$

where $M_{i,j}$ and $\text{Eff}_{i,j}$ is the particle number and collection efficiency for the ith particle diameter and the jth minute, respectively, and ρ_{p} is the particle density.

3. Numerical method

Numerical simulation was conducted to further explore the particle behavior inside the porous foam of the impactor and find out particle collection mechanism by the porous foam during the impaction process. To calculate particle penetration of the impactor, the flow field in the impactor was simulated by solving the 2D Navier–Stokes equations in the cylindrical coordinate. The fluid flow in the impactor was assumed steady, incompressible and laminar. Air was assumed to be at 20 °C and 1 atm. The governing equation was discretized by means of the finite volume method and solved by the SIMPLE algorithm (Patankar, 1980). The flow field is governed by

$$\rho(\vec{V} \bullet \vec{\nabla})\vec{V} = -\vec{\nabla}P + \mu\nabla^2\vec{V} - K\mu\vec{V}. \tag{5}$$

In Eq. (5), $\vec{V}$ is the velocity vector in m/s; P is the pressure in N/m^2; ρ is the air density in kg/m^3; μ is the air viscosity in N-s/m^2; K is the resistance factor of the porous substrate in m^{-2} ($K = 1/k$, k is the permeability). The resistance factor of the porous foam was measured experimentally and found to be $1.95 \times 10^8\ \text{m}^{-2}$. After obtaining the flow field, the particle equations of motion were solved numerically to obtained particle trajectories. The particle equations of motion in the r (radial) and z (axial) directions are:

$$\frac{\text{d}U_{\text{p}r}}{\text{d}t} = C_{\text{d}} Re_{\text{p}} \frac{\pi\mu D_{\text{p}}}{8Cm_{\text{p}}}(U_r - U_{\text{p}r}), \tag{6}$$

$$\frac{\text{d}U_{\text{p}z}}{\text{d}t} = C_{\text{d}} Re_{\text{p}} \frac{\pi\mu D_{\text{p}}}{8Cm_{\text{p}}}(U_z - U_{\text{p}z}) + g. \tag{7}$$

In the above equations, C_{d} is the empirical drag coefficient; Re_{p} is the particle Reynolds number; D_{p} is the particle diameter in m; m_{p} and g are particle mass and the gravitational acceleration in g and m/s^2, respectively; U_r and U_z are local flow velocities in the radial and axial directions in m/s, respectively; $U_{\text{p}r}$ and $U_{\text{p}z}$ are particle velocities in m/s, respectively. Grid independence checks were performed using different grid spacings. These checks revealed that approximately 40,000 grids were necessary to obtain a grid independent solution. As the particle equations of motion were integrated through the domain of interest, the new particle position and velocity after a small increment of time were calculated by numerical integration.

The particle penetration of the impactor with porous foam, P_{impactor}, can be defined as

$$P_{\text{impactor}} = \{1 - [R_{\text{in}} \times (1 - P_{\text{PF}})]\} \times 100\%, \tag{8}$$

where R_{in} is the ratio of particles impacted on top of the porous foam to those entering the nozzle of the impactor; and P_{PF} is the particle penetration of the porous foam. That is, R_{in} is the collection efficiency

of a solid-plate impactor while $1 - P_{PF}$ is the collection efficiency of the porous foam. P_{PF} can be found once $P_{impactor}$ and R_{in} are known. $P_{impactor}$ is the impactor penetration data from Eq. (3). The ratio R_{in} can be calculated as

$$R_{in} = [Y_{in}/(W/2)]^2, \tag{9}$$

where W is the nozzle diameter (m) and Y_{in} is the critical radial position (m) of the nozzle which demarcates the starting radial position for a particle to be collected by the substrate. Y_{in} can be calculated by the current numerical method based on the assumption that particle concentration and velocity profiles are uniform at the entrance of the nozzle.

After obtaining the particle penetration of the porous foam, P_{PF}, for the impactor with $W = 0.36$ cm at different sampling flow rates, non-linear multivariable regression was then used to obtain the following empirical equation based the form similar to Vincent, Aitken, and Mark (1993) as

$$P_{PF} = -0.026 + 1.026 \Big/ \left[1 + 0.00059 \frac{t}{D_f}(1.30044 St_p + 0.56187 Ng_p)^{1.8074}\right], \tag{10}$$

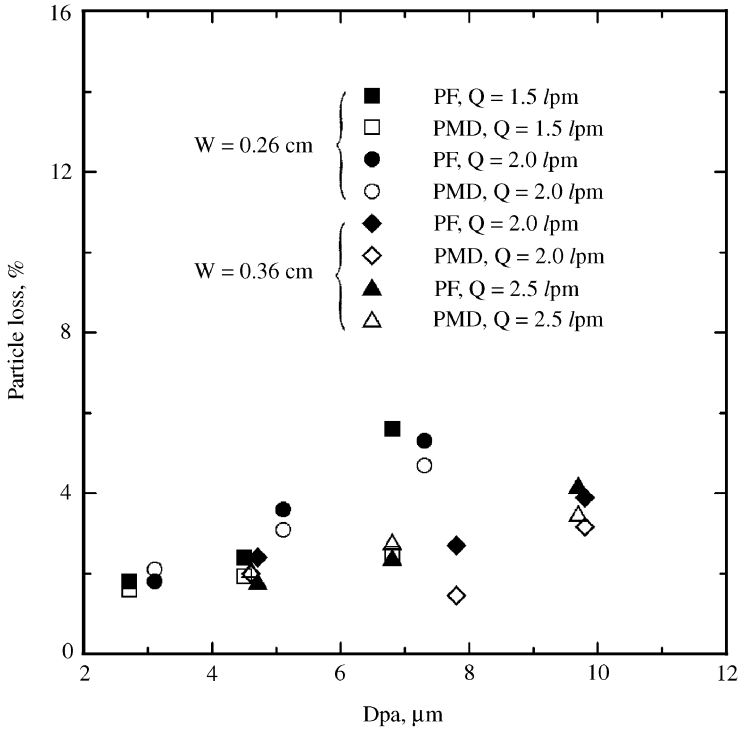

Fig. 3. Particle loss of the impactor with porous foam (PF) and porous metal disc (PMD) as the substrate at different flow rates (PF: 100 ppi, PMD: 20 μm in pore size).

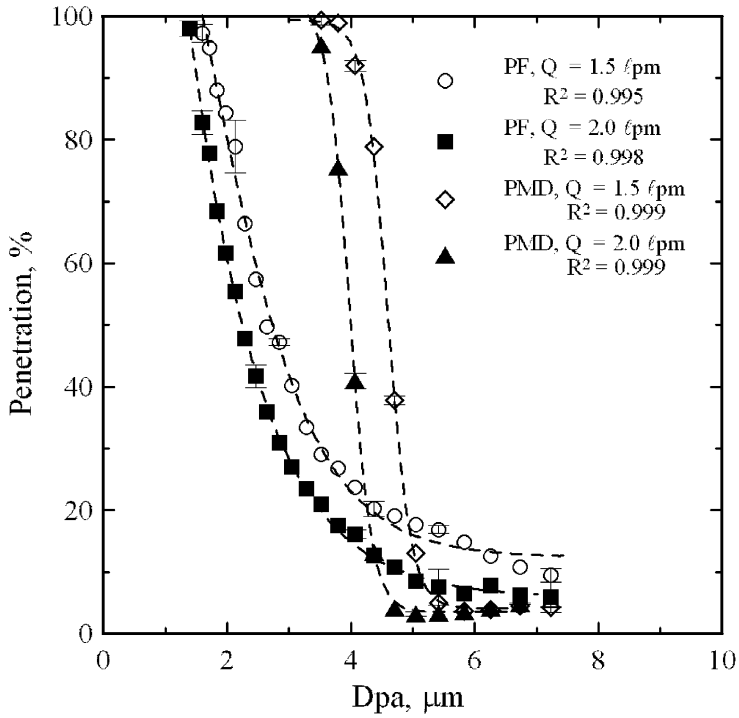

Fig. 4. Liquid particle penetration of the impactor with porous foam (PF) and porous metal disc (PMD) as the substrate, the nozzle diameter: 0.26 cm (PF: 100 ppi, PMD: 20 μm in pore size).

where t is the thickness of the porous foam in m; D_f is the equivalent fiber diameter of the porous foam in m. In Eq. (10), the Stokes' number St_p and the gravitational settling parameter Ng_p are defined as

$$D_f = 0.009633 \times \text{ppi}^{-1.216}, \tag{11}$$

$$St_p = \frac{\rho_p D_p^2 C U_0}{18\mu D_f}, \tag{12}$$

$$Ng_p = \frac{D_p^2 g C}{18\mu U_0}, \tag{13}$$

where ρ_p is the particle density in kg/m^3; U_0 is the average flow velocity at the impactor nozzle in m/s; and ppi is the pores per inch for the porous foam.

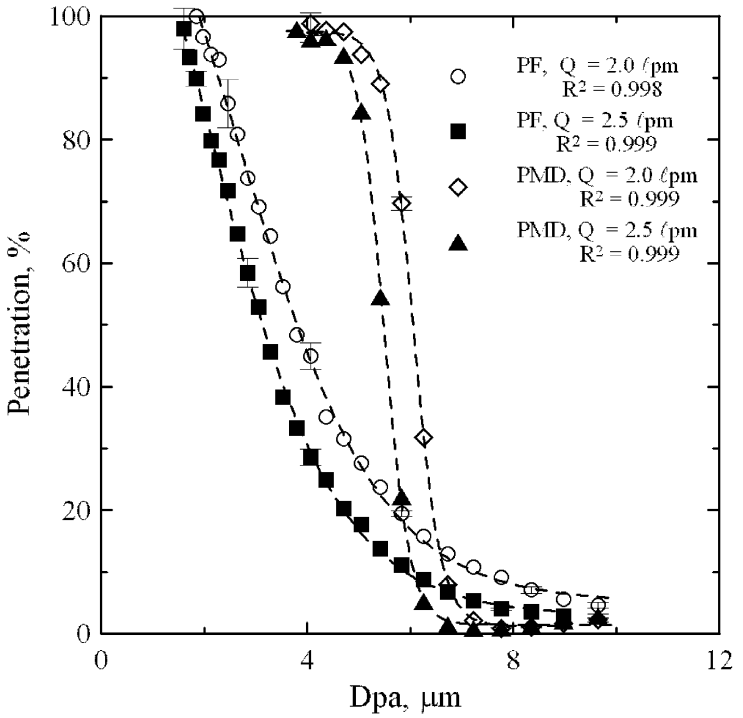

Fig. 5. Liquid particle penetration of the impactor with porous foam (PF) and porous metal disc (PMD) as the substrate, the nozzle diameter: 0.36 cm (PF: 100 ppi, PMD: 20 μm in pore size).

4. Results and discussion

4.1. Experimental data of particle penetration

Particle loss in the impactor was first measured using liquid oleic acid particles and the results are shown in Fig. 3. The aerodynamic diameter of the generated particle is 2.7, 3.1, 4.5, 5.1, 6.8, 7.3, 7.8, and 9.8 μm, respectively. Fig. 3 indicates that the maximum particle loss in the impactor is 4.2% for the nozzle diameter of 0.36 cm, and 5.6% for the nozzle diameter of 0.26 cm. It is seen that particle loss increases slightly with an increasing particle size, due to inertial impaction of larger particles. Particle loss is expected to be smaller for smaller particle diameter. Since particle loss is small, subsequent penetration measurement using the TSI APS must be accurate.

Figs. 4 and 5 show the liquid (oleic acid) particle penetration of the impactor for the nozzle diameter of 0.26 and 0.36 cm, respectively, at different sampling flow rates. The figures indicate that the penetration curve of the impactor with porous foam is different from that of with porous metal disc. For smaller particle diameter ($D_{pa} < 4.2$ μm for $W = 0.26$ cm and $D_{pa} < 6.6$ μm for $W = 0.36$ cm) at $Q = 2.0$ l/min, the particle penetration with porous foam is smaller than that with porous metal disc. This is because the resistance factor of the porous foam is smaller than the porous metal disc ($K = 1.95 \times 10^8$ and 6.87×10^{10} m^{-2} for the porous foam and the porous metal disc, respectively). As a result, more air penetrates into the porous foam and more particles are collected. On the contrary, for larger particle diameter ($D_{pa} > 4.2$ μm in Fig.

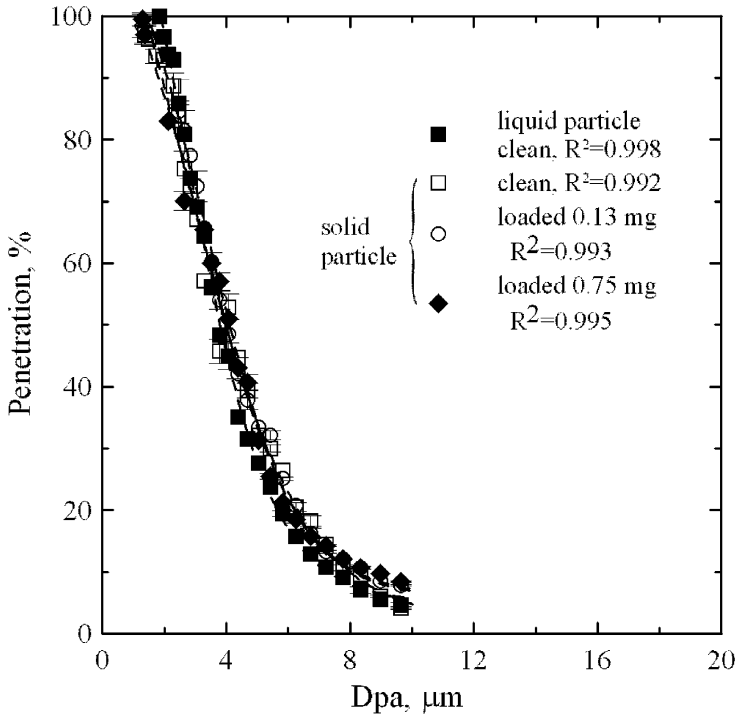

Fig. 6. Solid and liquid particles penetration of the impactor with porous foam (PF: 100 ppi) as the substrate at the various loaded mass for the nozzle diameter of 0.36 cm and $Q = 2.0$ l/min.

4 and $D_{pa} > 6.6\,\mu$m in Fig. 5) at $Q = 2.0$ l/min, particle penetration for the impactor with porous foam is higher than that with porous metal disc. This is because of poorer collection efficiency of coarse particles by the porous foam (Chen, Lai, Shih, & Yeh, 1998; Kavouras & Koutrakis, 2001) compared to that by the porous metal disc, despite that more air penetrates into the former than the latter.

In general, penetration curves of the impactor with porous foam are less sharp than those with porous metal disc, and the cutoff aerodynamic diameter of the former is less than that of the latter. For example, the cutoff aerodynamic diameter of the impactor with porous foam is 3.82 and 3.14 μm at $Q = 2.0$ and 2.5 l/min for $W = 0.36$ cm, and 6.05 and 5.48 μm for the impator with porous metal disc, respectively. Figs. 4 and 5 also show that the penetration of the impactor with porous foam and porous metal disc decreases with an increasing sampling flow rate. This is because more air flow penetrates into the porous substrate at higher sampling flow rate resulting in higher particle collection efficiency.

Fig. 6 shows the solid (KCl) particle penetration of the impactor with the porous foam for the nozzle diameter of 0.36 cm and the sampling flow rate of 2.0 l/min. It indicates that solid particle penetration curve of the impactor with porous foam is very close to that of liquid particle. The results show that particle bounce from the PF substrate can be avoided. Fig. 6 also shows that there is no obvious change in particle penetration curve when the particle loaded mass is increased to about 0.75 mg (7.37 mg/cm^2, particle loaded mass/deposited area), which is equivalent to 260 μg/m^3 for a 24-h sampling at 2 l/min. That is, the loading capacity of the porous foam in the impactor is sufficient enough for a long sampling time. These results are consistent with previous study using polyurethane foam as the substrate of an impactor

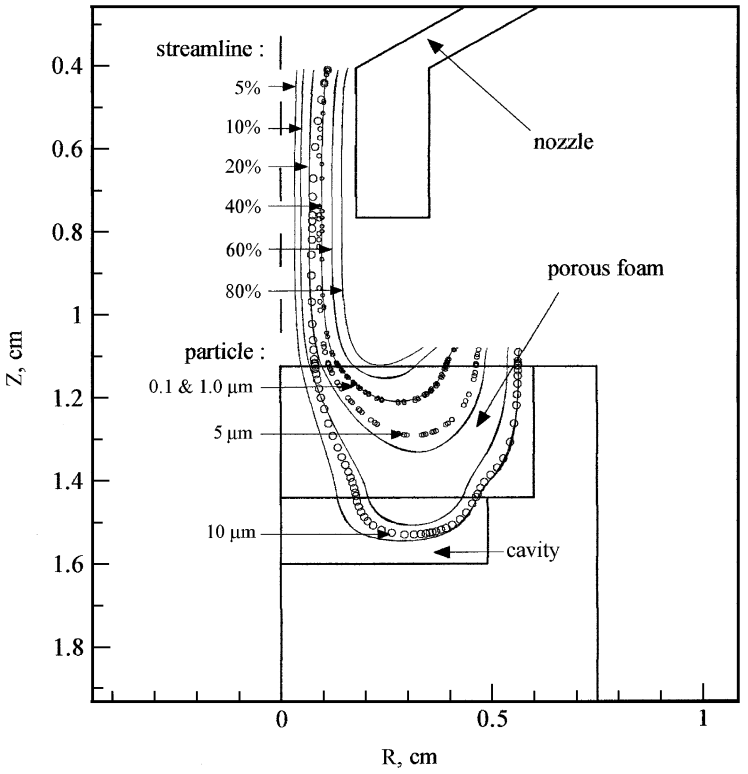

Fig. 7. Particle trajectories and streamlines of the impactor with porous foam. Nozzle diameter: 0.36 cm, flow rate: 2 l/min.

(Demokritou et al., 2004) with a sampling flow rate of 16.7 l/min. Their results showed that polyurethane foam substrate maintained adequate collection efficiency at a loading of at least 35 mg (82.77 mg/cm^2, particle loaded mass/deposited area).

4.2. Streamlines and particle trajectories

To investigate further the penetration characteristic of the porous foam substrate, streamline and particle trajectory in the impactor were simulated numerically. Fig. 7 illustrates particle trajectories and streamlines for the nozzle diameter of 0.36 cm at the flow rate of 2 l/min. The boundaries of the nozzle wall and the impaction cup were considered as solid. It is seen that streamlines inside the porous foam curve up due to the resistance of the substrate. For the case of a streamline position close to the centerline of the nozzle (streamline at 5%), the penetrating air travels longer distance inside the substrate than the position far away from the centerline of the nozzle (streamline at 60%). Further away from the centerline of the nozzle (streamline at 80%), air flow will not penetrate into the porous foam; therefore, small particles with insufficient inertia force will not be collected. Particle trajectories of different particle diameters starting at the same radial position corresponding to 40% of the total flow are also shown in Fig. 7. It is seen that trajectories of small particles ($D_p = 0.1$ and 1.0 μm) are close to air streamlines because of their small inertia. For particles with large particle diameters ($D_p = 5.0$ and 10.0 μm), trajectories

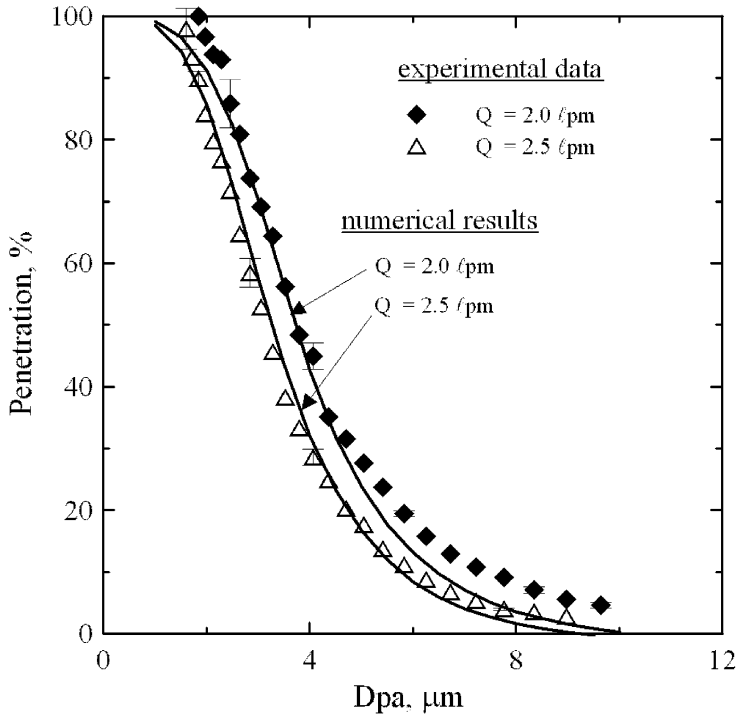

Fig. 8. Comparison of the numerical penetration curves of the impactor with porous foam with the experimental data for the liquid particle.

deviate from the corresponding streamlines due to inertia. Larger particles will be collected more easily inside the porous substrate due to inertial impaction and gravitational settling. Therefore, the penetration efficiency of smaller particles approaches 100% because they are apt to follow the streamlines to leave the porous foam. On the contrary, the penetration efficiency for larger particles approaches 0%, due to deviation of particle trajectories from streamlines and particles are eventually collected by the porous foam.

4.3. Comparison of numerical results with experimental data

Comparison of simulated penetration efficiencies with experimental data is shown in Fig. 8 for nozzle diameter of 0.36 cm at different sampling flow rates. It is seen that the numerical results are close to the experimental data. The numerical method was then used to predict penetration curves at other flow rates so that the flow rate that best matches the respirable sampling criteria can be found. Results are shown in Fig. 9 where the respirable curve (Hinds, 1999) is also plotted for comparison. It is seen that the penetration of the impactor with porous foam increases as the sampling rate is decreased due to less air penetration into the porous foam and smaller particle filtration efficiency by the porous foam. The figure also indicates when the nozzle diameter is 0.36 cm and the sampling flow rate is 1.9 l/min, the penetration curve of the impactor is very close to the respirable curve. The cutoff aerodynamic diameter and the slope of the penetration curve (slope $= \sqrt{D_{p16}/D_{p84}}$, $D_{p16\%}$ and $D_{p84\%}$: the diameter of particle

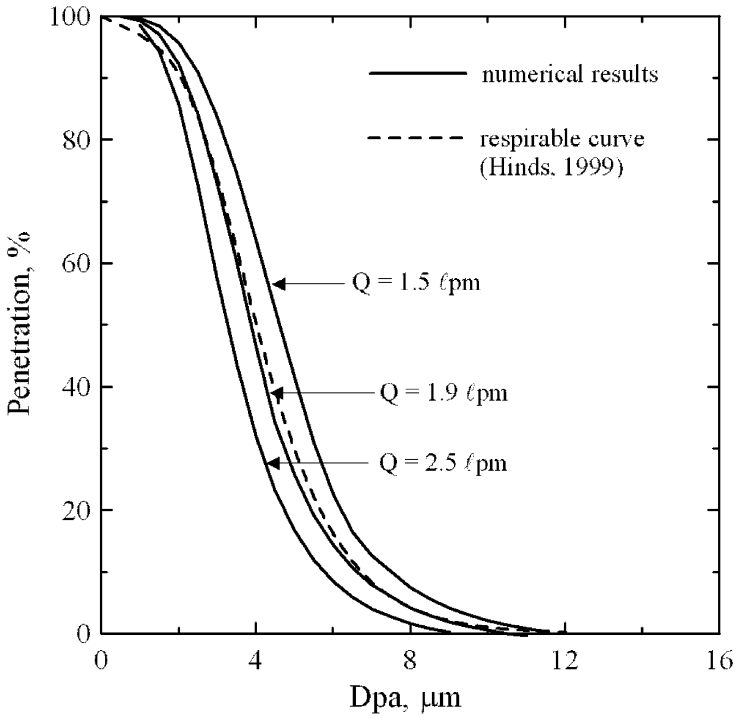

Fig. 9. Comparison of the penetration curves of the impactor with porous foam at different flow rates and the respirable sampling curve.

with 16% and 84% penetration) are found to be 3.9 μm (2.5% lower than that in the respirable curve, 4.0 μm) and 1.526 (1.9% lower than that in the respirable curve, 1.556), respectively. Therefore, the porous foam can be used as the collection substrate of a single nozzle inertial impactor for respirable aerosol sampling.

5. Conclusions

Traditionally cyclones have been used for respirable aerosol sampling because their penetration curves are much less sharp than those of impactors. This study has demonstrated that it is possible to use the porous foam as the substrate of a single nozzle impactor for respirable aerosol sampling. Experimental results show that penetration curves of the impactor with porous foam are less sharp than those with porous metal disc, and the cutoff aerodynamic diameter of the former is less than that of the latter. Test results show that solid particle bounce from the PF substrate can be avoided and there is almost no change in particle penetration efficiency curve when particles are loaded on the PF substrate.

Numerical results of particle penetration curves were validated by the experimental data and the method was then used to find the best sampling flow rate of the impactor with porous foam of 100 ppi for matching the respirable penetration curve. Results show that porous foam can be used as the collection substrate of

the inertial impactor (nozzle diameter: 0.36 cm) at the best flow rate of 1.9 l/min for respirable aerosol sampling.

Acknowledgements

The authors would like to thank for the support of the Taiwan National Science Council of the Republic of China under the Contract number NSC 92-2211-E-264-005, and the support of the Taiwan Institute of Occupational Safety and Health under the Contract number IOSH93-A304.

References

Chen, C. C., Lai, C. Y., Shih, T. S., & Yeh, W. Y. (1998). Development of respirable aerosol samplers using porous foams. *American Industrial Hygiene Association Journal*, *59*, 766–773.

Cohen, B. S., & Hering, S. V. (1995). *Air sampling instruments*. Cincinnati: American Conference of Governmental Industrial Hygienists Inc.

Demokritou, P., Kavouras, I. G., Ferguson, S. T., & Koutrakis, P. (2002). Development of a high volume cascade impactor for toxicological and chemical characterization studies. *Aerosol Science and Technology*, *36*, 925–933.

Demokritou, P., Lee, S. J., & Koutrakis, P. (2004). Development and evaluation of a high loading PM2.5 speciation sampler. *Aerosol Science and Technology*, *38*, 111–119.

Hinds, W. C. (1999). *Aerosol technology*. New York: Wiley.

Huang, C.-H., & Tsai, C.-J. (2003). Mechanism of particle impaction and filtration by the dry porous metal substrates of an inertial impactor. *Aerosol Science and Technology*, *37*, 486–493.

Huang, C.-H., Tsai, C.-J., & Shih, T.-S. (2001). Particle collection efficiency of an inertial impactor with porous metal substrates. *Journal of Aerosol Science*, *32*, 1035–1044.

Kavouras, I. G., Ferguson, S. T., Wolfson, J. M., & Koutrakis, P. (2000). Development and validation of a high volume low cut-off inertial impactor (HVLI). *Inhalation Toxicology*, *12*, 35–50.

Kavouras, G., & Koutrakis, P. (2001). Use of polyurethane foam as the impaction substrate/collection medium on conventional inertial impaction. *Aerosol Science and Technology*, *34*, 46–56.

Lilienfeld, P., & Dulchinos, J. (1972). Portable instantaneous mass monitor for coal mine dust. *American Industrial Hygiene Association Journal*, *33*, 136–145.

Marjamaki, M., & Keskinen, J. (2004). Experimental study on the effect of impaction plate porosity and roughness on impactor collection efficiency. *Journal of Aerosol Science*, *35*, 301–308.

Marple, V. A. (1978). Simulation of respirable penetration characteristics by inertial impaction. *Journal of Aerosol Science*, *9*, 125–134.

Marple, V. A., & McCormack, J. E. (1983). Personal sampling impactor with respirable aerosol penetration characteristics. *American Industrial Hygiene Association Journal*, *44*, 916–922.

Patankar, S. V. (1980). *Numerical heat transfer and fluid flow*. Washington, DC: Hemisphere.

Tomb, T. F., & Treaftis, H. N. (1975). A new two-stage respirable dust sampler. *American Industrial Hygiene Association Journal*, *36*, 1–9.

Tsai, C.-J., Huang, C.-H., Wang, S.-H., & Shih, T.-S. (2001). Design and testing of a personal porous metal denuder. *Aerosol Science Technology*, *35*, 611–616.

Tsai, C.-J., Shiau, H.-G., Lin, K.-C., & Shih, T.-S. (1999). Effect of deposited particles and particle charge on the penetration of small sampling cyclones. *Journal of Aerosol Science*, *30*, 313–323.

Vincent, J. H., Aitken, R. J., & Mark, D. (1993). Porous plastic foam filtration media: Penetration characteristics and applications in particle size-selective sampling. *Journal of Aerosol Science*, *24*, 929–944.

Willeke, K., & Haberman, S. A. (1980). Inclined-surface impaction for respirable particle sampling. *Atmospheric Environment*, *14*, 1109–1111.